Selenium-mediated arsenic excretion in mammals: a synchrotron-based study of whole-body distribution and tissue-specific chemistry

Olena Ponomarenko,[a¶] Paul F. La Porte,[bcd¶] Satya P. Singh,[a] George Langan,[e] David E.B. Fleming,[f] Julian E. Spallholz,[g] Mohammad Alauddin,[h] Habibul Ahsan,[i] Selim Ahmed,[j] Jürgen Gailer,[k] Graham N. George*[al] and Ingrid J. Pickering,*[al]

a. *Molecular and Environmental Science Research Group, Department of Geological Sciences, University of Saskatchewan, Saskatoon, Saskatchewan S7N 5E2, Canada. E-mail: g.george@usask.ca, ingrid.pickering@usask.ca*
b. *Pritzker School of Medicine, University of Chicago, Chicago, IL 60637, USA*
c. *Emory University School of Medicine, Emory University, Atlanta, GA 30322, USA*
d. *Division of Hematology-Oncology, University of California Los Angeles, CA 90095, USA*
e. *Department of Surgery, University of Chicago, Chicago, IL 60637, USA*
f. *Department of Physics, Mount Allison University, Sackville, NB, E4L 1E6, Canada*
g. *Nutritional Sciences, Texas Tech University, Lubbock, TX 79409 , USA*
h. *Chemistry Department, Wagner College, Staten Island, NY 10301, USA*
i. *Department of Health Sciences, University of Chicago, Chicago, IL 60637, USA*
j. *School of Medicine, University Malaysia Sabah, Sabah 88400, Malaysia*
k. *Department of Chemistry, University of Calgary, Calgary, AB, T2N 1N4 Canada*
l. *Department of Chemistry, University of Saskatchewan, Saskatoon, SK, S7N 5C9, Canada*

* *Corresponding Authors*

¶ *These authors contributed equally to this work.*

Contents

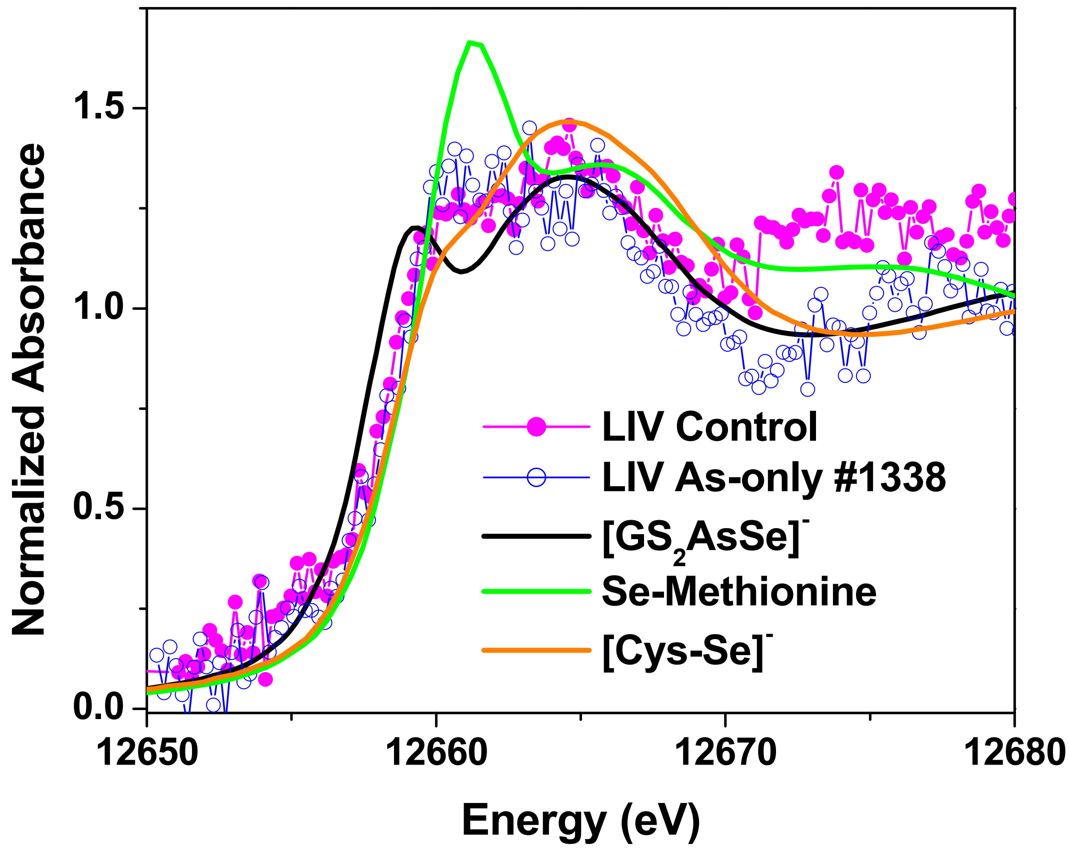

Fig. S1 Se K X-ray absorption near-edge spectra: frozen liver tissue from a control animal dosed with sham (magenta, solid circles); frozen liver tissue from As-only dosed animal, specimen #1338 (blue, open circles); selenocysteine (Cys-Se⁻) standard solution (orange); selenomethionine standard solution (green); seleno *bis*-(S-glutathionyl) arsinium anion standard (black).

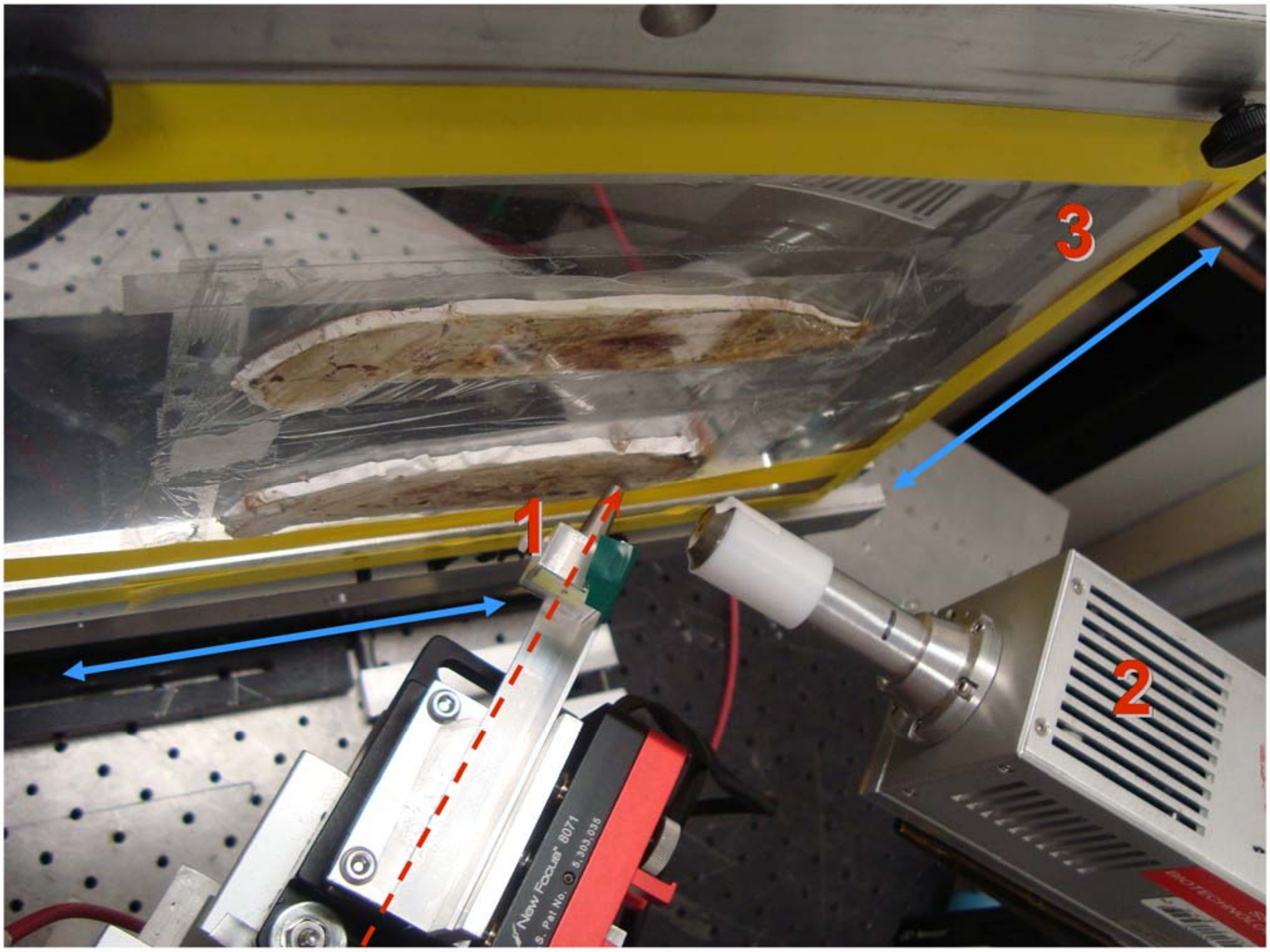

Fig. S2 The experimental configuration for wide-format synchrotron X-ray fluorescence imaging at the Stanford Synchrotron Radiation Laboratory (SSRL) beamline 10-2 showing hamster specimens mounted on the stage (view from above). Synchrotron X-rays at 13.450 keV (denoted by the red dashed arrow) were focused through a polycapillary optic (1). A Vortex detector (2) was positioned at a 90° angle to the incident beam. The lyophilized slices were mounted vertically on a motorized stage (3) at 45° to the incident X-ray beam and raster scanned in the beam. The blue double-ended solid arrow denotes the vertical and horizontal movement directions of the motorized stage.

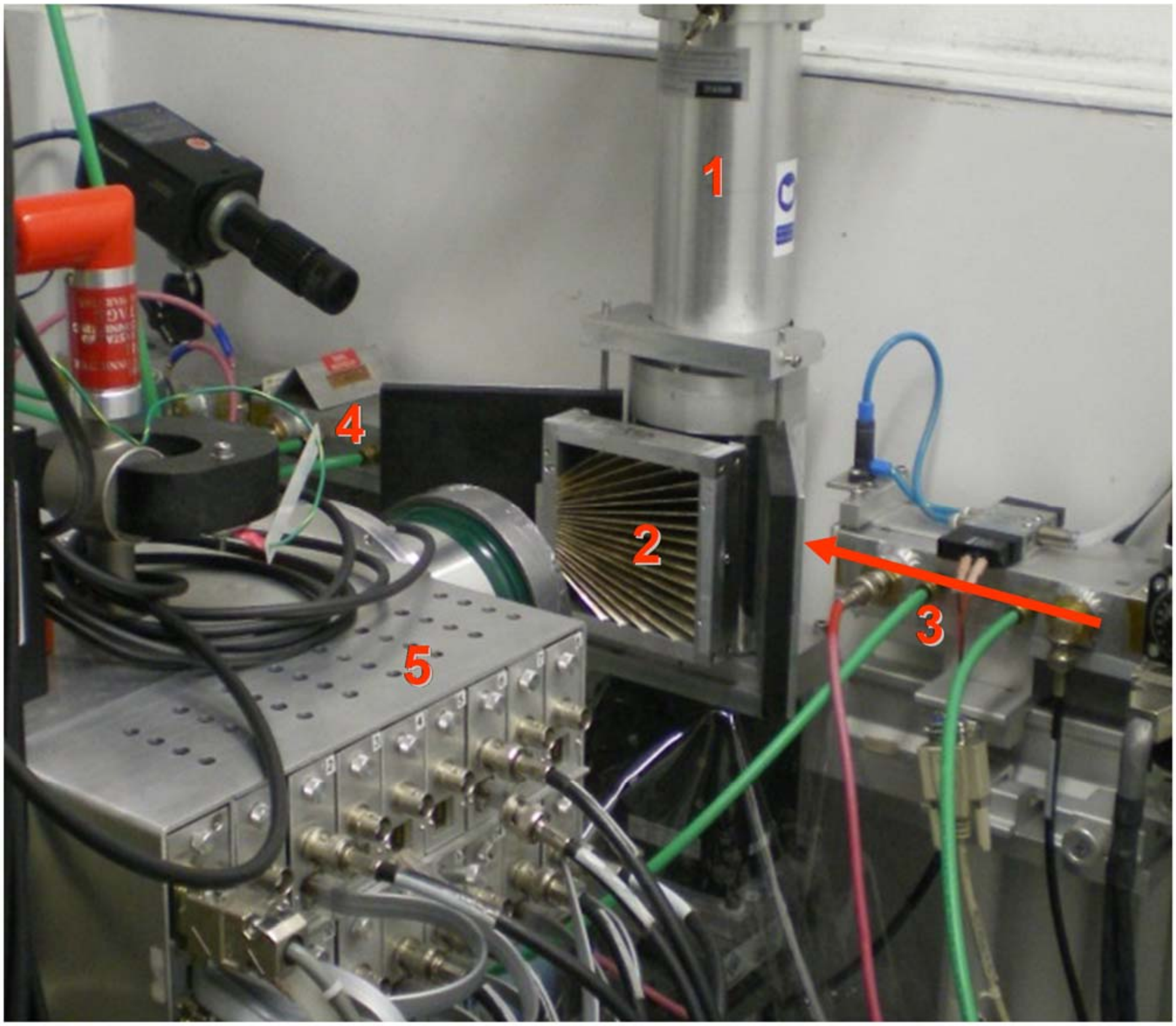

Fig. S3 The experimental configuration for bulk X-ray absorption spectroscopy (XAS) analysis of frozen hamster tissues at SSRL beamline 7-3. The arrow denotes the synchrotron beam direction. 1- continuous flow liquid helium cryostat (Oxford Instruments), 2- Soller slits, 3- and 4- upstream and downstream ionization chambers, 5 - 30-element Ge solid-state detector (Canberra).

Calculations of elemental concentrations using explicitly non-finite thickness and absorption properties of samples in the standard method

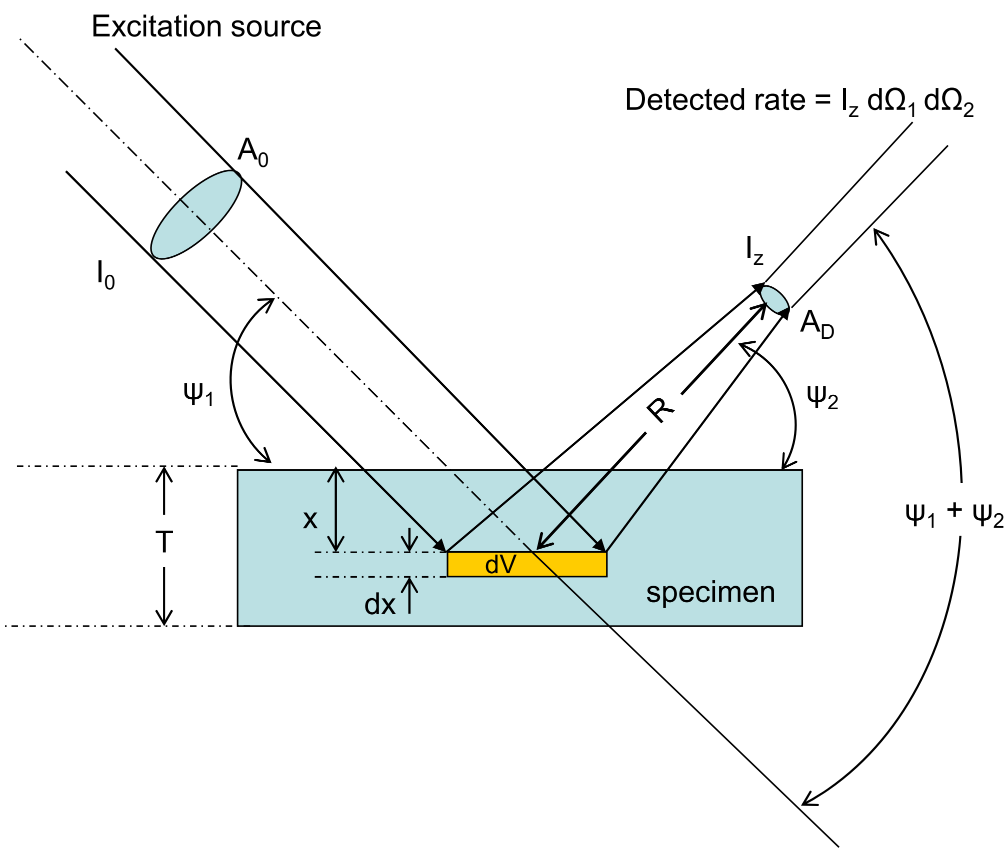

Fig. S4 Geometry for derivation of the primary fluorescence intensity (adapted from [1, 2])

The derivation is based on the approach of Jenkins, Gould and Gedcke[1] and Sparks[2] with the following simplifications (see also a recent review by Pushie *et al.*[3]):

1) We consider a monochromatic incident X-ray beam of energy E_0 and intensity I_0;

2) Only emission of characteristic X-rays from a specific line (say, $K\alpha$) of the element z is considered.

σ_0 is the total mass attenuation coefficient [cm^2/g] for the specimen at energy E_0 and ρ [g/cm^3] is the density of the specimen; σ_i is the total mass attenuation coefficient [cm^2/g] for the specimen at the characteristic X-ray radiation of energy E_i .

In Figure S4, ψ_1 and ψ_2 are defined as the incident and outgoing (takeoff) angles, respectively. The number of photons per second emitted by the monochromatic excitation source for the energy E_0

within the differential solid angle $d\Omega_1$ is defined by $I_0(E_0)d\Omega_1$. The photons strike the surface of the specimen at an incidence angle ψ_1. The fluoresced photon beam is emitted toward the detector into the differential solid angle $d\Omega_2$ at an outgoing angle ψ_2.

It is necessary to calculate the number of characteristic X-rays of energy E_i fluoresced in the differential element of thickness dx, located at the distance x behind the specimen surface. In order to reach this volume element, the incident X-rays must pass through an effective specimen thickness $x\csc\psi_1$. As the result of absorption along this path length, the rate of photons arriving at the differential volume is reduced to:

$$I_1(E_0) = I_0(E_0)\exp[-\sigma_0 \rho x \csc\psi_1]d\Omega_1 \quad \text{(SI.1)}$$

The emitted photon rate in the analyzed line in the differential element of thickness dx is:

$$I_F(E_i) = W_z \sigma_{zki}(E_0) I_1(E_0) \rho dx \csc\psi_1 \quad \text{(SI.2)}$$

where $\sigma_{zki}(E_0)$ is the fluorescence cross section for a particular line i of electron shell k for the element of interest z; W_z is the weighted fraction (equivalently, the mass concentration) of the element z in the sample. The characteristic photon radiation is emitted in all directions into a solid angle of 4π steradians. The fraction of the photon rate emitted toward the detector into the differential solid angle $d\Omega_2$ at an outgoing angle ψ_2 is proportional to $\frac{d\Omega_2}{4\pi}$. If σ_i is the total mass attenuation coefficient [cm^2/g] for the specimen at the characteristic X-ray radiation of energy E_i, then before emerging from the specimen following the path length $x\csc\psi_2$, the characteristic photon rate will be attenuated. The detected characteristic photon rate for the differential solid angles $d\Omega_1$ and $d\Omega_2$ (see Figure S4) from the differential volume element of thickness dx located at the distance x behind the specimen surface, taking in account the detector efficiency $\eta(E_i)$ for the line i is defined as:

$$\begin{aligned} I_F(E_i)dx\,d\Omega_1 d\Omega_2 &= \eta(E_i)\times \\ &\times \underbrace{W_z \sigma_{zkj}(E_0) I_0(E_0)\exp[-\sigma_0 \rho x \csc\psi_1]\rho dx \csc\psi_1}_{\text{the rate of characteristic radiation generated in the slab dx}} \times \underbrace{\exp[-\sigma_i \rho x \csc\psi_2]}_{\text{attenuation of characteristic radiation}} \times d\Omega_1 \frac{d\Omega_2}{4\pi} \quad \text{(SI.3)} \end{aligned}$$

To obtain the contribution from the entire specimen thickness, we have to integrate (SI.3) over the range $x = 0$ to $x = T$ and over the finite solid angles Ω_1 and Ω_2. Using $\csc\psi = \frac{1}{\sin\psi}$ and re-arranging the result we obtain:

$$I_i(E_i)=\frac{1}{4\pi}Q_i(E_0,\eta(E_i),\Omega_1,\Omega_2)\times W_z\sigma_{zki}(E_0)\times$$
$$\times\left(\frac{1-\exp\left\{-\frac{\rho T}{\sin\psi_1}\left[\sigma(E_0)+\sigma(E_i)\frac{\sin\psi_1}{\sin\psi_2}\right]\right\}}{\sigma(E_0)+\sigma(E_i)\frac{\sin\psi_1}{\sin\psi_2}}\right)\times I_0(E_0) \qquad \text{.......(SI.4)}$$

where the term $Q_i(E_0,\eta(E_i),\Omega_1,\Omega_2)$ is a factor which depends on the geometry of the source and detector, the detector efficiency for the line *i*, and absorption of the fluorescent radiation from element *z* due to its path from the sample surface to detector.

Frequently, data libraries for X-ray absorption of different materials report the X-ray *length attenuation* $\mu(E)$ [cm^{-1}] or *attenuation length* $\mu(E)^{-1}$ [cm]. The total length attenuation of the specimen $\mu(E)$ for energy *E* is related to the mass attenuation via $\sigma(E)=\mu(E)/\rho$. In terms of length attenuation, the weight concentration (weight fraction) W_z of the element *z* in grams per 1 gram of the sample weight may be found, using (SI.4), as:

$$W_z=Q_i'(E_0,E_i,\eta(E_i),\sigma_{zki}(E_0),\Omega_1,\Omega_2,)\times$$
$$\frac{I_i}{I_0}\times\frac{\left(\mu_0+\mu_i\frac{\sin\psi_1}{\sin\psi_2}\right)\Big/\rho}{\left\langle 1-\exp\left\{-\left[\left(\mu_0+\mu_i\frac{\sin\psi_1}{\sin\psi_2}\right)\Big/\rho\right]\rho T/\sin\psi_1\right\}\right\rangle} \qquad \text{.......(SI.5)}$$

where we introduce the combined coefficient,

$Q_i'(E_0,E_{i,}\eta(E_i),\sigma_{zki}(E_0),\Omega_1,\Omega_2)=1/[4\pi\times Q_i(E_0,\eta(E_i),\Omega_1,\Omega_2)\times\sigma_{zki}(E_0)]$,

which includes the fluorescence cross-section $\sigma_{zki}(E_0)$. In the *fundamental parameter* method, the coefficient should be determined, either in experiments or theoretically. In our case, the *standard method* was employed. This coefficient can be found by measuring the intensity of fluorescent radiation using the same experimental setup for a standard of known concentration $W^{st}{}_z$, density ρ_{st}, and thickness *t*:

$$Q'(E_0,E_i,\eta(E_i),\sigma_{zki},\Omega_1,\Omega_2)_z=\frac{\langle 1-\exp\{-A_{st}\rho_{st}t/\sin\psi_1\}\rangle}{A_{st}}\times\frac{I_0{}^{st}{}_z}{I_i^{st}}\times W^{st}{}_z \qquad \text{.......(SI.6)}$$

Here A_{st} is *the combined effective mass-absorption coefficient*

$$A_{st}=(\mu_{s0}+\mu_{si}\sin\psi_1/\sin\psi_2)/\rho_{st} \qquad \text{.......(SI.7)}$$

I_0^{st} and $I_i^{st}{}_z$ are, respectively, the mean rates of incident radiation of energy E_0 and characteristic photon radiation of energy E_i of element *z* in the standard for the particular line *i*.

The areal density $\widetilde{C}^{st}{}_z$ [g/cm²] of a standard is defined as the mass of a standard per unit area, $S_1 = 1\ cm^2$. It can be related to the density of the standard via its thickness *t* (in *cm*) as

$$\widetilde{C}^{st}{}_z = \rho_{st} \times t \left[g / cm^2\right] \qquad \text{(SI.8)}$$

For standards or a simple sample matrix, software for calculation of mass attenuation (mass absorption cross sections) based on McMaster's tables[4] is readily available[5]. However, for more complex samples, experimentally determined tabulated mass absorption cross sections (or length attenuation coefficients) may be obtained from sources such as NIST[6] or CXRO[7]; see Tables S1-S2 below.

The weight concentration (or, alternatively, areal density) of elements of interest in a sample of known density and thickness could be obtained by combining Eq. (SI.5) and Eq. (SI.6 – SI.8), together with absorption cross-sections for the elements of interest, for the sample matrix and the standards. This algorithm was programmed in Matlab code for the pixel-by-pixel calculation of the elemental concentrations in the lyophilized animal sections.

Parameters for calculation of concentrations

The average thickness *T* [cm] for each of the hamster sections was obtained by caliper measurements at 6 locations along the section, two locations in each of the shoulder/head region, the lung/diaphragm region and the lower abdomen/pelvis region of the body section. The total area *S* [cm²] of each animal section was calculated by summing pixels with non-background intensity in the Zn image. Zn is abundant in all animal tissues and provides a very high contrast marker for the body section area compared with the background of the mylar support. The density *ρ* of the hamster sections was determined by weighing the sections and dividing the mass *m* [g] of each section by its measured volume, $\rho = m/(S \times T)$ [g/cm³]. The average density obtained this way for the lyophilized sections was *0.40 ± 0.005* [g/cm³]. This value compared well with the density of lyophilized chicken meat found in the literature, *ρ(high porosity chicken meat, freeze-dried) = 0.41* [g/cm³].[8] This density value was used to calculate the mass attenuation coefficient (absorption cross section) *σ* [cm²/g] from tabulated length attenuation coefficients found on-line for fresh animal soft tissues with corrections for water content. Knowing that soft tissues have ~ 70% of water content, we use the following formula:

$$\left(\frac{\mu}{\rho}\right)_{fresh} = \sum_i \omega_i \left(\frac{\mu}{\rho}\right)_i = \left(1 - \omega_{water}\right)\left(\frac{\mu}{\rho}\right)_{dried-matter} + \omega_{water}\left(\frac{\mu}{\rho}\right)_{water} \qquad \text{(SI.9)}$$

The tabulated data are presented in Tables S1 – S2.

Table S1 Mass attenuation values (absorption cross sections) for the incident energy 13.45 keV and for K_α fluorescent characteristic energies of the elements of interest for relevant media

Energy reference	Energy, [keV]	Mylar,[a,e] μ/ρ [g/cm^2]	H_2O,[b] μ/ρ [g/cm^2]	fresh muscle,[c] μ/ρ [g/cm^2]	dried muscle[d], H_2O-corrected, μ/ρ [g/cm^2]
Ca K_α	3.69168	70.171	78.606	99.433	148.028
Mn K_α	5.89875	16.779	22.810	25.379	31.370
Fe K_α	6.40384	13.018	18.363	19.976	23.738
Cu K_α	8.04778	6.414	10.045	10.265	10.776
Zn K_α	8.63886	5.149	8.331	8.350	8.392
As K_α	10.5437	2.790	4.923	4.672	4.085
Se K_α	11.2224	2.309	4.176	3.896	3.241
Incident beam	13.450	1.352	2.589	2.298	1.620

[a] Mylar film[4, 7]; [b] water[6]; [c] fresh muscle tissue[6]; and [d] dried muscle corrected for water content using Eq. SI.9. [e] Since 6.3 µm thick metal-free mylar film covered both the samples and the standards, the absorption due to the mylar top layer can be included in the coefficient (Eq. SI.6) and does not need to be calculated separately; nevertheless the values of mass absorption cross section are included here for completeness.

Table S2 Mass attenuation values (absorption cross sections) for the incident energy 13.45 KeV and for K_α fluorescent characteristic energies of the elements of interest[4, 7]

Element	Standard compound	Mass (areal) density [µg/cm^2]	Density, [g/cm^3]	Concentration fraction [g/g]	Element's K_α energy [keV]	μ/ρ [g/cm^2] at element's K_α energy	μ/ρ [g/cm^2] at incident energy (13450 eV)
Ca	CaF_2	56.8	3.18	0.51	3.69168	154.12	22.29
Mn	Mn	47.1	7.3	1	5.89875	74.21	67.29
Fe	Fe	56.0	7.874	1	6.40384	68.09	76.32
Cu	Cu	49.3	8.96	1	8.04778	50.07	100.00
Zn	ZnTe	45.8	7.133	0.34	8.63886	167.26	82.63
As	GaAs	47.3	5.316	0.52	10.54372	121.61	125.05
Se	Se	46.4	4.5	1	11.2224	50.54	11.27

Table S3 Microelement and trace element concentration means (μ) and standard deviations (σ) in μg/g (dry weight) in tissues of hamster slice specimens

		Ca		Mn		Fe		Cu		Zn		As		Se	
		μ	σ	μ	σ	μ	σ	μ	σ	μ	σ	μ	σ	μ	σ
control *	liver	49.0	61.0	11.8	19.3	215.2	64.2	2.8	0.7	16.0	2.3	0.1	0.2	6.8	2.2
	heart	58.0	19.0	7.2	6.1	202.1	161.0	3.5	1.4	14.0	3.9	0.1	0.2	1.8	1.4
	lung	57.0	27.0	7.6	5.8	321.2	136.0	1.6	1.3	8.7	3.8	0.1	0.2	1.7	1.4
	throat	183.0	509.0	3.4	3.8	77.6	83.8	0.9	0.9	16.0	7.4	0.1	0.2	1.4	1.2
	int 1	189.0	191.0	89.3	103.0	74.7	52.4	3.5	3.3	23.0	14.0	0.1	0.3	1.3	1.2
	int 2	157.0	249.0	60.8	98.0	70.5	54.3	2.5	3.3	22.0	13.0	0.1	0.3	1.3	1.2
Se-only †	liver 1	70.0	43.0	14.2	9.2	192.9	83.0	2.8	1.3	21.0	6.4	0.3	0.8	157.9	47.0
	liver 2	79.0	65.0	13.6	7.4	198.0	47.9	3.2	1.1	20.0	3.6	0.3	0.7	164.4	18.0
	heart	91.0	72.0	6.0	5.9	100.2	56.2	3.8	1.2	15.0	2.8	0.2	0.6	149.2	25.0
	lung	99.0	38.0	15.8	10.4	323.1	129.0	0.7	0.4	8.0	2.4	0.3	0.8	56.7	18.0
	throat	209.0	357.0	6.4	9.0	104.8	138.0	0.6	0.7	11.0	8.3	0.2	0.5	14.5	9.8
	int 1	227.0	366.0	53.4	92.4	89.5	80.5	3.6	5.1	22.0	20.0	0.4	1.0	22.2	17.0
	int 2	173.0	197.0	36.8	54.1	71.0	67.0	2.1	2.4	17.0	10.0	0.3	0.7	20.3	12.0
As-only ‡	liver 1	18.0	14.0	15.2	8.1	145.3	47.0	1.5	0.7	7.7	2.4	100.7	24.6	2.8	2.0
	liver 2	82.0	194.0	19.3	12.5	170.1	70.4	1.3	0.7	7.7	2.3	85.6	27.3	2.0	1.7
	heart	31.0	27.0	11.7	8.5	124.3	74.5	1.6	0.8	6.5	2.7	23.9	7.7	0.7	1.0
	lung	25.0	14.0	18.8	10.0	212.0	77.5	0.9	0.7	4.3	1.9	22.7	6.2	0.6	0.9
	throat	208.0	617.0	3.8	4.8	34.1	22.2	0.7	0.5	12.0	3.9	13.4	6.0	0.6	0.9
	int 1	70.0	118.0	31.2	46.0	94.7	57.4	1.3	1.7	6.6	6.5	36.7	24.9	0.7	1.0
	int 2	79.0	237.0	14.6	29.1	44.5	25.7	0.9	1.0	5.3	3.8	80.0	70.3	0.6	1.2
As-only §	bile duct	22.3	23.7	11.5	8.5	100.3	56.9	1.8	1.0	11.9	3.4	251.4	78.8	7.6	5.4
	liver 1	15.5	14.7	15.5	9.0	151.9	58.8	2.1	1.0	15.2	4.5	153.2	71.0	6.1	5.4
	liver 2	21.1	25.6	17.0	8.6	160.2	42.9	2.0	0.8	12.8	2.7	203.4	39.2	6.5	4.6
	heart	67.6	279.4	10.0	9.5	102.4	77.8	1.7	1.1	12.7	5.2	53.7	29.5	1.5	2.2
	lung	19.3	26.5	13.6	8.8	155.5	51.6	1.1	0.8	11.0	2.6	92.0	33.6	2.6	3.1
	throat	40.8	170.6	8.2	9.8	91.5	94.5	0.7	0.6	9.9	5.0	30.0	13.6	1.4	2.0
	int 1	35.6	64.2	17.9	26.8	41.2	38.3	1.6	1.7	10.4	7.7	61.5	42.8	1.4	2.4
	int 2	23.9	51.0	8.7	10.9	40.0	30.5	1.0	0.8	8.8	4.1	88.6	110.7	1.3	2.4
	muscle	117.5	380.8	2.4	3.3	19.9	15.1	0.8	0.7	19.5	8.5	10.9	6.8	1.0	1.8
As & Se ¶	liver 1	180.5	328.7	19.1	32.5	127.1	56.7	2.7	1.4	19.4	5.4	166.7	102.6	22.1	14.6
	liver 2	135.0	411.9	11.6	8.6	167.1	99.0	2.0	1.1	15.6	5.3	151.0	82.0	29.5	17.6
	heart	125.9	117.5	7.4	6.6	130.6	82.1	3.1	1.2	13.6	3.5	83.4	14.4	9.6	6.1
	lung	154.0	357.4	18.8	8.9	400.8	87.5	1.0	0.7	8.3	1.6	90.4	22.2	28.6	9.0
	throat	122.4	148.5	4.9	5.7	73.1	70.2	0.8	0.9	13.0	7.7	25.3	14.8	6.2	6.0
	int 1	199.8	184.4	47.8	72.6	84.4	47.9	2.2	2.6	15.5	11.9	48.4	44.0	5.1	4.8
	int 2	360.1	250.6	63.8	65.2	104.0	43.3	2.8	2.0	13.9	10.0	14.7	14.4	2.0	2.5
As & Se #	bile duct	59.7	29.1	7.0	4.9	50.1	38.0	1.4	0.5	10.7	2.3	355.2	175.0	413.8	243.8
	liver 1	77.7	37.2	6.8	5.6	65.5	30.2	1.9	0.9	10.6	2.3	227.5	70.6	311.5	94.1
	liver 2	123.4	162.0	31.8	51.8	145.5	73.0	3.0	1.8	17.4	8.1	90.6	49.3	85.3	45.3
	heart	270.6	788.5	7.4	9.3	116.8	139.5	0.9	0.9	7.9	6.0	13.9	9.1	17.2	10.6
	lung	47.3	20.0	15.8	8.5	327.0	110.1	0.9	0.6	8.9	3.2	19.9	9.0	30.4	9.3
	throat	99.3	105.9	3.5	4.1	47.5	49.9	0.9	1.1	8.1	6.9	7.2	6.7	10.4	8.3
	int 1a	139.5	293.4	21.3	40.7	128.8	102.6	1.4	1.7	10.3	8.4	48.0	66.9	55.4	92.4
	int 1b	149.8	306.6	22.9	42.4	136.4	104.2	1.4	1.8	10.6	8.6	35.4	41.8	35.8	36.3
	int 2	56.0	31.6	8.9	5.7	79.4	27.5	1.4	0.7	10.3	2.9	243.2	54.4	350.3	137.0
	muscle	72.9	45.9	3.2	3.7	46.4	18.8	1.7	0.8	18.1	3.8	7.4	4.1	13.5	6.0
	brain	449.3	1034.9	1.9	3.1	19.0	6.9	1.9	0.8	15.6	4.0	0.8	1.1	4.3	2.4

[*] control, sham dosing; [†] dosed with Se only (specimen #1341); [‡] dosed with As only (specimen #1340); [§] dosed with As only (specimen #1338); [¶] dual dosing with As:Se = 5:1 (specimen #1337); [#] dual dosing with As:Se = 1:1 (specimen #1335)

Table S4 Reference arsenic- and selenium-containing compounds used in the least-squares fitting of X-ray absorption spectroscopy data

Compound	Formula[a]
Arsenate	$As^{V}O(OH)_2O^-$
Arsenite	$As^{III}(OH)_3$
arsenic(III) *tris*-glutathione	$As^{III}(SG)_3$
monomethylarsonous acid [MMA(III)]	$CH_3As^{III}(OH)_2$
monomethylarsonic acid [MMA(V)]	$CH_3As^{V}O(OH)_2$
dimethylarsinic acid [DMA(V)]	$(CH_3)_2As^{V}O(OH)$
trimethylarsine oxide	$(CH_3)_3As^{V}O$
Trimethylarsine	$(CH_3)_3As^{III}$
(2-methyl-1,3,2-*di*-thiarsinan-4-yl)pentanoic acid	$CH_3As^{III}S_2Lip$
Seleno-*bis*(S-glutathionyl) arsinium ion	$[(GS)_2As^{III}Se]^-$
Selenate	$[Se^{VI}(OH)O_3]^-$
Selenite	$[Se^{IV}(OH)O_2]^-$
L-selenomethionine	$CH_3Se(CH_2)_2CH(NH_2)CO_2^-$
Selenocysteinylcysteine	(Cys)SeS(Cys)[b]
Seleno-*di*-glutathione	GS-Se-SG
Selenocysteineate	$SeCH_2CH(NH_2)CO_2^-$
Trimethylselenonium ion	$[(CH_3)_3Se]^+$

[a] Glutathione, γ-*L*-glutamyl-*L*-cysteinylglycine, is abbreviated in the table as GSH. In all cases the coordination to arsenic or selenium is via the cysteine thiolate moiety. In many cases, ionizable groups are present and the species given is the majority at pH 7.5. Selected near-edge XAS spectra of these compounds are shown in our recent paper on observation of $[(GS)_2AsSe]^-$ in rat bile.[9]

[b] In this case the abbreviation (Cys) is used to indicate the non chalcogenide fragment of selenocysteine or cysteine, *i.e.* $^-$[—$CH_2CH(NH_2)CO_2^-$].

References

1 R. Jenkins, R. W. Gould and D. Gedcke, *Quantitative X-ray Spectrometry*, Marcel Dekker, Inc, New York, 2nd edn., 1995.

2 C. J. Sparks, in *Synchrotron Radiation Research*, eds. H. Winick and S. Doniach, Plenium Press, New York, 1980, ch. 14, pp. 459–512.

3 M. J. Pushie, I. J. Pickering, M. Korbas, M. J. Hackett and G. N. George, Elemental and Chemically Specific X-ray Fluorescence Imaging of Biological Systems, *Chem. Rev.*, 2014, **114**, 8499–8541.

4 W. H. McMaster, N. Kerr Del Grande, J. H. Mallett and J. H. Hubbell, Compilation of X-Ray Cross Sections. Lawrence Livermore National Laboratory Report, National Technical Information Services L-3, US Dept. of Commerce, 1969.

5 G. N. George and I. J. Pickering, A suite of computer programs for analysis of X-ray Absorption Spectra, 2000, SSRL/SLAC, http://ssrl.slac.stanford.edu/~george/exafspak/manual.pdf, (accessed June 2017).

6 J. H. Hubbell and S. M. Seltzer, Tables of X-Ray mass attenuation coefficients and mass energy-absorption coefficients from 1 keV to 20 MeV for elements Z = 1 to 92 and 48 Additional substances of dosimetric interest, NIST, https://www.nist.gov/pml/x-ray-mass-attenuation-coefficients, (accessed June 2017).

7 The Center for X-Ray Optics, X-Ray Database, http://henke.lbl.gov/optical_constants/, (accessed June 2017).

8 B. E. Farkas and R. P. Singh, Physical properties of air-dried and freeze-dried chicken white meat, *J. Food Sci.*, 1991, **56**, 611–615.

9 G. N. George, J. Gailer, O. Ponomarenko, P. F. La Porte, K. Strait, M. Alauddin, H. Ahsan, S. Ahmed, J. E. Spallholz and I. J. Pickering, Observation of the seleno bis-(S-glutathionyl) arsinium anion in rat bile, *Inorganic Biochemistry*, 2016, **158**, 24–29.